Energy Efficient Adaptive Transmissions in Integrated Satellite-Terrestrial Networks With SER Constraints

Yuhan Ruan[ID], Yongzhao Li, *Senior Member, IEEE*, Cheng-Xiang Wang[ID], *Fellow, IEEE*, and Rui Zhang[ID], *Member, IEEE*

Abstract—**Allowing frequency reuse between satellite and terrestrial networks, the integrated satellite-terrestrial network can spatially optimize the usage of scarce spectrum resource and is thus becoming one of the most promising infrastructures for future multimedia services. Taking the requirements of both efficiency and reliability in satellite communications into account, we propose an adaptive transmission scheme for the integrated network in this paper, where the satellite can communicate with the destination user either in direct mode or in cooperative mode. Specifically, we first investigate the symbol error rate (SER) performance of two transmission modes with co-channel interference under composite multipath/shadowing fading. Taking the derived SERs as constraints, we formulate the adaptive transmission scheme as an optimization problem with the objective of maximizing energy efficiency (EE) and discuss the trade-off among EE, spectral efficiency (SE), and SER. Furthermore, economic efficiency is also analyzed as a complementary performance measure to SE and EE. Simulation results show that the proposed scheme can increase the attainable EE of satellite communications, which indicates that we should choose the transmission mode adaptively according to different interfering scenarios and shadowing degrees, rather than adopting cooperative transmission aggressively.**

Index Terms—**Integrated satellite-terrestrial networks, adaptive transmission, symbol error rate, energy efficiency, economic efficiency.**

I. INTRODUCTION

SATELLITE systems have been commonly applied in the context of broadcasting, navigation, rescue, and disaster relief due to its characteristic of wide coverage. One potential

drawback is that the system degrades in the presence of shadowing, occurring when the line-of-sight (LOS) link between the satellite and the terrestrial user is blocked by obstacles. While the cellular network can provide low-cost coverage for high-density populations in urban areas through its non-line-of-sight (NLOS) communication. It can be seen that a/an hybrid/integrated satellite-terrestrial cooperative network comprising a satellite component and a terrestrial component that complement each other can realize genuine ubiquitous communication [1], [2]. In this case, the mobile user can exploit the advantage of spatial diversity gain by receiving independent fading signals from the satellite and terrestrial relays. As a result, a higher transmission rate and/or more reliable transmission can be achieved [3], [4].

In a hybrid network, terrestrial components operate independently from the satellite and do not necessarily operate in the same frequency band as the satellite. Until now, numerous studies have been done on the hybrid satellite-terrestrial cooperative network (HSTCN) from various performance metrics, such as symbol error rate (SER) [5] and outage probability (OP) [6] in single-antenna scenarios. Extension works to multi-antenna satellite communications with orthogonal space-time block coding (OSTBC) and beamforming schemes were conducted in [7] and [8], respectively. Moreover, some studies explored performance of the HSTCN from the perspective of relay selection or power allocation with various objectives. Sreng *et al.* [9] selected the relay with the best quality of the relay-destination link in a single-user scenario. Taking the reliability of transmission as target, Upadhyay and Sharma [10] employed a max-max user-relay selection scheme to minimize the OP of the system. Despite of the benefits of the hybrid network, the independence between satellite and terrestrial components in a hybrid network cannot meet the increasing demand for higher spectral efficiency (SE) of the overall system.

To address this issue, the integrated satellite-terrestrial network which spatially optimizes the usage of scarce spectrum resource was introduced in [11], and is becoming an attractive and promising infrastructure for future multimedia services. Different from the hybrid network, the integrated satellite-terrestrial network is a system employing mobile satellite service (MSS) and a terrestrial component where the terrestrial component is complementary to and operates as part of the MSS system. In the integrated network, the terrestrial segment is controlled by the satellite resource and

network management system. Further, the terrestrial component uses the same designated portions of the frequency band as the associated operational MSS system. Although the frequency reuse between satellite and terrestrial components can increase the SE of the overall system, it would inevitably cause co-channel interference, referred as inter-component interference [12]. In this regard, Deslandes *et al.* [13] presented several interference scenarios and evaluated the influence of the satellite frequency reuse pattern and the exclusion zone size. Interference mitigation schemes based on position and dynamic resource allocation were studied in [14] and [15], respectively. Moreover, An *et al.* [16] and Yang and Hasna [17] conducted performance evaluations of an amplify-and-forward (AF) based integrated satellite-terrestrial network with co-channel interference corrupting both the relay and destination nodes. In addition, fifth-generation (5G) communications are also involved in the integration of satellite and terrestrial networks. B.S.M.R. *et al.* [18] analytically evaluated the self-interference and co-channel interference in a scenario where full-duplex enabled small cells reuse the satellite feeder uplink band. In [19], low power device-to-device (D2D) transmission mode was employed by terrestrial communication systems to access the satellite spectrum band.

The aforementioned papers [5], [6], [16], and [17] mainly focused on performance analysis of the hybrid/integrated satellite-terrestrial network adopting the cooperative transmission mode aggressively, without considering whether the added relay node could achieve performance enhancement in practical implementation. Actually, in the frequency reuse case, cooperative transmission is not always more efficient than the direct transmission when taking interference and circuit power consumption into account. Based on the observation in [20], it is meaningful to adopt different transmission modes contingently. However, to the best of the authors' knowledge, an adaptive transmission scheme has not been studied in the integrated satellite-terrestrial network, where the interference environment and channel fading are different from terrestrial networks. Moreover, the existing studies mainly optimized the performance of satellite communications from a single perspective, such as SER in [5] and [17], capacity in [16], energy efficiency (EE) in [21], OP in [9] as well as our previous work [6], [22], without considering the interrelationship among these performance metrics. To fill the above research gaps, we introduce an energy efficient adaptive transmission scheme for integrated satellite-terrestrial networks with SER constraints, where the terrestrial component uses the same portions of the mobile satellite system frequency bands [23]. Note that in the integrated satellite-terrestrial networks we focus on in this paper, the terrestrial component the satellite and terrestrial components are integrated from the physical layer aspect.[1] In this situation, the satellite can communicate

with the destination either directly (direct mode) or employing the terrestrial component as a repeater to achieve cooperative diversity (cooperative mode). The major contributions of this paper can be summarized as follows:

- To optimize the utilization of network resources, an adaptive transmission scheme for the integrated satellite-terrestrial network is proposed for the first time, illustrating the optimally energy efficient transmission mode for different interfering scenarios with various shadowing degrees.

- We extend the scenario of the integrated satellite-terrestrial network in [16] and [17] to a more practical one, where multipath fading and shadowing fading are all considered for the satellite downlinks and terrestrial links. For such a composite multipath/shadowing fading environment, we model all links as generalized-K fading channels uniformly for its relatively simple mathematical form [23]. Based on which, theoretical analyses of the exact SERs and asymptotic SERs are conducted for two transmission modes.

- Taking the requirements of both efficiency and reliability in satellite communications into account [25], [26], we analyze the trade-off among SE, SER, and EE. Specifically, taking the derived SERs as constraints, we optimize the EE of satellite communications to obtain the optimal transmission mode. Moreover, we discuss the effect of SER constraints on the optimal transmission mode from the perspective of EE-SE trade-off. Furthermore, the economic efficiency (ECE) is evaluated as a complementary performance measure to SE and EE, offering an inherent trade-off between SE and EE.

The remainder of the paper is organized as follows. Section II introduces the system model. Section III investigates the SER performance of the integrated satellite-terrestrial network. In Section IV, an energy efficient adaptive transmission scheme is proposed. Simulation and numerical results are given in Section V. Finally, conclusions are given in Section VI.

II. System Model

As illustrated in ETSI TR 103 124 v1.1.1, there are multiple ways in combining satellite and terrestrial communications. The integrated and hybrid satellite terrestrial networks are two popular ways in the existing literature. The main difference between integrated and hybrid systems is on whether both space and terrestrial parts use a common network and spectrum. The terrestrial part of an integrated system is a complementary part of the satellite system and thus, it uses the same frequency band allocated to the satellite system and is operated by the same network. On the other hand, a hybrid system may combine a satellite system with a terrestrial one with different frequency bands, networks, and even air interfaces.

Considering the integrated system can spatially optimize the usage of scarce spectrum resource, in this paper, we consider an integrated satellite-terrestrial network as shown in Fig. 1, where the satellite component and terrestrial components operate on the same frequency band (L band or S band)

---

[1]As described in ETSI TR 103 124 v1.1.1, satellite and terrestrial components can be integrated either at lower layer (e.g., in [24] where cooperative diversity technique was employed in physical layer) or at higher layer (e.g., in BATS project where traffic was dynamically routed between the terrestrial based internet access and the satellite broadband access and then recombined at application layer). In this paper, we concentrate on signal processing and resource allocation at lower layer as in [23].
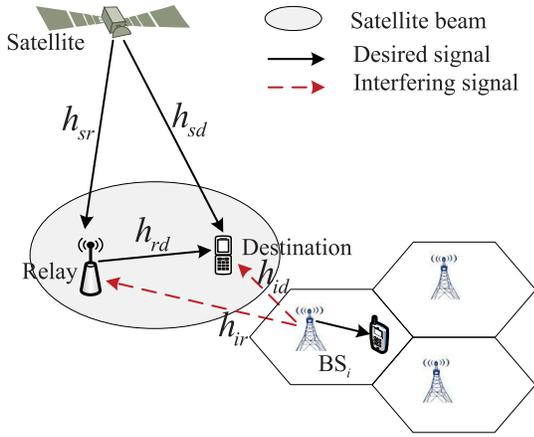
Fig. 1.   System model of the integrated satellite-terrestrial network.

and use a common management system. In the integrated network, the satellite (S) communicates with the destination terminal (D) either directly or employing the terrestrial relay station (R) as a repeater to achieve spatial diversity gains.[2] Related resource allocation scheme will be detailed in Section IV and this process can be carried out at the level of gateway or the network control center. It is assumed that each node is equipped with a single antenna and operates in a half-duplex mode. Due to the frequency reuse, the relay and/or the destination will suffer from the interference caused by cellular i-th base station ($BS_i, i = 1, \cdots, L$). We denote h_{sr}, h_{sd}, and h_{rd} as the channel coefficients of S $\rightarrow$ R, S $\rightarrow$ D, and R $\rightarrow$ D communication links, respectively, while h_{ir} and h_{id} as the channel coefficients of $BS_i \rightarrow$ R and $BS_i \rightarrow$ D interfering links, respectively.[3]

A. Signal Models of Two Transmission Modes

1) The Direct Mode: In the direct mode, the satellite transmits signal to the destination directly with power P_s. Meanwhile, the destination will suffer from the interference from the surrounding base stations, each of which the transmit power is P_I. The signal received at the destination can be expressed as

$$y_{sd} = \sqrt{P_s}h_{sd}x + \sum_{i=1}^{i=L} \sqrt{P_I}h_{id}z + n_d \qquad (1)$$

where x is the desired signal from the satellite and z is the interfering signal from the base stations. Herein, n_d is the noise at the destination in the direct mode. It is assumed that all the noises in this paper are complex additive white Gaussian noises (AWGNs) each with power N_0. The signal-to-interference-plus-noise ratio (SINR) for the direct mode, γ_{sd}, can be expressed as

$$\gamma_{sd} = \frac{P_s|h_{sd}|^2}{\sum_{i=1}^{i=L} P_I|h_{id}|^2 + N_0} = \frac{\gamma_1}{\gamma_2 + 1} \qquad (2)$$

[2]In this paper, we concern the physical transmission performance and thus, the cooperation between the satellite and the terrestrial relay we focus on falls into the physical layer to obtain spatial diversity gains. Here, the terrestrial relay relies on the existing cellular infrastructure.

[3]These channels are assumed to be quasi-static and channel information can be obtained by adopting the channel estimation method proposed in [27].

where $\gamma_1 = P_s|h_{sd}|^2/N_0 = \bar{\gamma}_s|h_{sd}|^2$ and $\gamma_2 = \sum_{i=1}^{i=L} P_I|h_{id}|^2/N_0 = \bar{\gamma}_I \sum_{i=1}^{i=L} |h_{id}|^2$. Here, $\bar{\gamma}_s$ and $\bar{\gamma}_I$ denote the average signal-to-noise ratio (SNR) of the satellite and interference-to-noise ratio (INR) of each base station, respectively.

2) The Cooperative Mode: In the cooperative mode, we focus on the physical cooperative transmission and the terrestrial relay is employed as a repeater to achieve spatial diversity gains. The whole transmission of the satellite communication consists of two orthogonal time phases and both the relay and the destination are corrupted by the interference. In the first phase, the satellite broadcasts its signal to the relay and the destination. The signals received at the relay and the destination can be written as

$$y_{sr} = \sqrt{P_s}h_{sr}x + \sum_{i=1}^{i=L} \sqrt{P_I}h_{ir}z + n_r \qquad (3)$$

and

$$y_{sd} = \sqrt{P_s}h_{sd}x + \sum_{i=1}^{i=L} \sqrt{P_I}h_{id}z + n_{d1} \qquad (4)$$

where n_r and n_{d1} are the noises at the relay and the destination in the first phase, respectively. After receiving signals from the satellite, the relay employs AF strategy to multiply all the received signals y_{sr} with a multiplication factor ρ and then forward it to the destination, where $\rho = 1/\sqrt{P_s|h_{sr}|^2 + \sum_{i=1}^{i=L} P_I|h_{ir}|^2 + N_0}$ is the energy normalized factor to satisfy the average transmit power constraint. By denoting P_r as the transmit power of the relay, the signal received at the destination can be obtained as

$$y_{rd} = \sqrt{P_sP_r}h_{sr}h_{rd}\rho x + \sqrt{P_r}h_{rd}\rho \sum_{i=1}^{i=L} \sqrt{P_I}h_{ir}z$$

$$+ \sum_{i=1}^{i=L} \sqrt{P_I}h_{id}z + \sqrt{P_r}h_{rd}\rho n_r + n_{d2} \qquad (5)$$

where n_{d2} is the noise at the destination in the second phase.

By assuming maximal ratio combining (MRC) employed at the destination, we have the instantaneous SINR for the cooperative mode as

$$\gamma_{coop} = \gamma_{sd} + \gamma_{srd} \qquad (6)$$

where γ_{sd} is the SINR for the satellite-destination link as expressed in (2) and γ_{srd} is the SINR for the satellite-relay-destination link. From (5) we can obtain

$$\gamma_{srd} = \frac{UV}{U + V + 1} \qquad (7)$$

where $U = \frac{\gamma_3}{\gamma_4+1}$ with $\gamma_3 = P_s|h_{sr}|^2/N_0 = \bar{\gamma}_s|h_{sr}|^2$ and $\gamma_4 = \sum_{i=1}^{i=L} P_I|h_{ir}|^2/N_0 = \bar{\gamma}_I \sum_{i=1}^{i=L} |h_{ir}|^2$, $V = \frac{\gamma_5}{\gamma_2+1}$ with $\gamma_5 = P_r|h_{rd}|^2/N_0 = \bar{\gamma}_r|h_{rd}|^2$. Similarly, $\bar{\gamma}_r$ denotes the average SNR of the relay node.

B. Channel Model

The most popular land mobile satellite (LMS) model is the Loo model [28], where the power of the LOS component is assumed to be log-normally distributed while the multipath component has a Rayleigh distribution. Since the log-normal distribution is involved, the Loo channel model is almost analytically intractable and some approximations have to be employed, which leads to non-rigorous analysis. Alternatively, a new LMS model was proposed in [29], where the log-normal distribution in Loo model is replaced by Gamma distribution. It has been shown that this new model provides a similar fit to the experimental data as the Loo model but with significantly less computational complexity. In this paper, the integrated satellite-terrestrial network shown in Fig. 1 involves in two LMS links ($S \rightarrow R$ and $S \rightarrow D$) and multiple terrestrial links ($R \rightarrow D$, $BS_i \rightarrow R$, and $BS_i \rightarrow D$). To make the analysis tractable, we model all links uniformly as the generalized-K distribution because of its relatively simple mathematical form that allows an integrated performance analysis of digital communication systems operating in composite multipath/shadowing fading environment. The generalized-K distribution is a mixture of Gamma-distributed shadowing and Nakagami-distributed multipath fading effect. As demonstrated in [30], the generalized-K model can not only properly describe the signal propagation on terrestrial links, but also the channel environment subjects to Loo model.

For the generalized-K model, the probability density function (PDF) of $|h|^2$ can be written as

$$f_{|h|^2}(x) = \frac{2b^{m_s+m_m}}{\Gamma(m_s)\Gamma(m_m)} x^{\left(\frac{m_s+m_m}{2}\right)-1} K_{m_s-m_m}\left(2b\sqrt{x}\right) \quad (8)$$

where $x > 0$, $K_{m_s-m_m}(\cdot)$ is the modified Bessel function of the second kind with order $(m_s - m_m)$ and $b = \sqrt{\frac{m_m m_s}{\Omega_0}}$. Here, $m_m \geq 0.5$ and $m_s \geq 0$ are the multipath parameter and the shadowing parameter, respectively, and Ω_0 is the mean of the received local power.

III. SER Performance Analysis

In this paper, we propose an energy efficient adaptive transmission scheme for the integrated network under SER constraints. In order to make SER a constraint when optimizing the transmission scheme for the integrated network, we investigate the SER performance of two transmission modes in this section firstly. We proceed from evaluating the exact SER in closed-form expressions, hereafter, by approximating the exact SERs at high SNR value, we obtain the asymptotic SERs in a linear form, which can be easily used as constraints to guarantee the reliability requirement of satellite communications.

A. Average SER

1) Direct Mode: For the direct mode, the average SER can be directly evaluated by averaging the conditional error probability over its corresponding PDF, such that [31]

$$\mathcal{P}_{dire} = \frac{1}{2\sqrt{2\pi}} \int_0^\infty \frac{e^{-\frac{y}{2}}}{\sqrt{y}} F_{\gamma_{sd}}\left(\frac{y}{\beta}\right) dy \quad (9)$$

where β is a constant depending on the modulation scheme and $F_{\gamma_{sd}}(x)$ is the cumulative distribution functions (CDF) of the received SINR γ_{sd}. Herein, $F_{\gamma_{sd}}(x)$ can be derived as

$$F_{\gamma_{sd}}(x) = 1 - \sum_{m=0}^{k_1-1} \frac{\lambda_1^m \lambda_2^{Lk_2}}{m! \bar{\gamma}_s^m \bar{\gamma}_I^{Lk_2}} \sum_{q=0}^{m} \binom{m}{q} (Lk_2)_q$$
$$\times x^m e^{-\frac{\lambda_1}{\bar{\gamma}_s}x} \left(\frac{\lambda_2}{\bar{\gamma}_I} + \frac{\lambda_1}{\bar{\gamma}_s}x\right)^{-Lk_2-q} \quad (10)$$

where $(u)_v = \Gamma(u+v)/\Gamma(u)$ is the Pochhammer symbol [32, p. xliii]. By substituting (10) into (9), $\mathcal{P}_{dire}$ can be obtained as

$$\mathcal{P}_{dire} = \frac{1}{2} - \frac{\sqrt{2}}{4\sqrt{\pi}} \sum_{m=0}^{k_1-1} \frac{\lambda_1^m \left(\frac{\lambda_1}{\bar{\gamma}_s\beta} + \frac{1}{2}\right)^{-m-\frac{1}{2}}}{\beta^m m! \bar{\gamma}_s^m \Gamma(Lk_2)} \sum_{q=0}^{m} \binom{m}{q} \frac{\bar{\gamma}_I^q}{\lambda_2^q}$$
$$\times G_{21}^{12}\left[\frac{2\lambda_1 \bar{\gamma}_I}{\lambda_2(2\lambda_1 + \bar{\gamma}_s\beta)} \left| \begin{matrix} \frac{1}{2} - m, 1 - Lk_2 - q \\ 0 \end{matrix} \right. \right] \quad (11)$$

where $\Gamma(\cdot)$ and $G_{p,q}^{m,n}[\cdot|\cdot]$ denote the Gamma function [32, eq. (8.310.1)] and the Meijer-G function [32, eq. (9.301)], respectively.

The derivation steps of $F_{\gamma_{sd}}(x)$ and $\mathcal{P}_{dire}$ can be found in Appendix A.

2) Cooperative Mode: The average SER of a cooperative communication system with M-ary phase-shift keying (M-PSK) modulation can be calculated as [31]

$$\mathcal{P}_{MPSK} = \frac{1}{\pi} \int_0^{\theta_M} M_\gamma\left(\frac{g_{MPSK}}{\sin^2\theta}\right) d\theta \quad (12)$$

where $\theta_M = \pi(M-1)/M$, $g_{MPSK} = \sin^2(\pi/M)$, and $M_\gamma(s)$ denotes the moment generating function (MGF) of the equivalent SINR. For a random variable γ, $M_\gamma(s)$ is defined as

$$M_\gamma(s) = \mathbb{E}\left\{e^{-s\gamma}\right\} = \int_0^\infty e^{-s\gamma} f_\gamma(\gamma) d\gamma \quad (13)$$

where $\mathbb{E}\{\cdot\}$ denotes the expectation operator. From $\gamma_{coop} = \gamma_{sd} + \gamma_{srd}$ and the definition of MGF in (13), we find the MGF of the sum of two independent variables can be calculated by the product of their own MGFs. Thus, we have

$$M_{\gamma_{coop}}(s) = M_{\gamma_{sd}}(s) M_{\gamma_{srd}}(s) \quad (14)$$

where $M_{\gamma_{sd}}(s)$ and $M_{\gamma_{srd}}(s)$ are the MGFs of γ_{sd} and γ_{srd}, respectively. After some algebraic manipulations, the analytical expressions for $M_{\gamma_{sd}}(s)$ and $M_{\gamma_{srd}}(s)$ can be given by

$$M_{\gamma_{sd}}(s) = \sum_{h=0}^{k_1} \binom{k_1}{h} \frac{\lambda_1^{k_1} \bar{\gamma}_I^h (s + \lambda_1/\bar{\gamma}_s)^{-k_1}}{\Gamma(Lk_2)\Gamma(k_1)\bar{\gamma}_s^{k_1}\lambda_2^h}$$
$$\times G_{21}^{12}\left[\frac{\lambda_1 \bar{\gamma}_I}{\lambda_2(\lambda_1 + \bar{\gamma}_s s)} \left| \begin{matrix} 1 - k_1, 1 - Lk_2 - h \\ 0 \end{matrix} \right. \right] \quad (15)$$

and

$$M_{\gamma_{srd}}(s) = 1 - \sum_{n=0}^{k_3-1} \frac{\lambda_3^n}{n!\bar{\gamma}_s^n} \sum_{l=0}^{N} \frac{(-1)^l}{l!} \left(\frac{\lambda_4\bar{\gamma}_s}{\lambda_3\bar{\gamma}_I}\right)^{Lk_4+l} \sum_{p=0}^{n}\binom{n}{p}$$
$$\times (Lk_4)_{l+p} \frac{\bar{\gamma}_s^p}{\lambda_3^p}\left(\frac{\lambda_2\bar{\gamma}_r}{\lambda_5\bar{\gamma}_I}\right)^{Lk_2} \frac{(Lk_2)_{k_5}s^{\tilde{p}+Lk_2}}{\Gamma(\tilde{p}+Lk_2+1)\Gamma(k_5)}$$
$$\times G_{22}^{22}\left[\frac{\bar{\gamma}_s s}{\lambda_3}\,\middle|\,\begin{matrix} -\tilde{p}, 1 \\ 1-\tilde{p}-Lk_2, Lk_2 \end{matrix}\right]. \tag{16}$$

The derivation steps of $M_{\gamma_{sd}}(s)$ and $M_{\gamma_{srd}}(s)$ can be found in Appendix B.

Then, by substituting (15) and (16) into (14), $M_{\gamma_{coop}}(s)$ can be obtained. In the subsequent derivation of average SER, there is no closed-form solution for the integral in (12). Alternatively, the following tight approximate expression can be used [36, eq. (30)]

$$\mathcal{P}_{coop} = \sum_{l=1}^{3} \xi_l M_{\gamma_{sd}}(\omega_l) M_{\gamma_{srd}}(\omega_l) \tag{17}$$

where $\xi_1 = \theta_M/(2\pi) - 1/6$, $\xi_2 = 1/4$, $\xi_3 = \theta_M/(2\pi) - 1/4$, and $\omega_1 = g_{MPSK}$, $\omega_2 = 4g_{MPSK}/3$, $\omega_3 = g_{MPSK}/\sin^2(\theta_M)$.

By substituting the expressions of $M_{\gamma_{sd}}(s)$ and $M_{\gamma_{coop}}(s)$ specified in (15) and (16) into (17), we can finally obtain the SER expression of the cooperative mode.

B. Asymptotic SER

Although the above analyses can provide exact performance evaluations, these results do not provide straight insights into the effects of different parameters on the performance of two transmission modes, e.g., the number of interferers and the interfering power. Moreover, we consider a SER constrained integrated satellite-terrestrial network, a linear form of the SER expression is needed for convenience. Thus, in what follows, we conduct an asymptotic analysis of SER at high SNR for the satellite communication.

1) Direct Mode: Using the series representation and asymptotic behavior of the incomplete Gamma function as [32, eq. (8.354.1)], we have

$$\Upsilon(s,x) = \sum_{n=0}^{\infty} \frac{(-1)^n x^{s+n}}{n!(s+n)} = \frac{x^s}{s} \quad (x \to 0). \tag{18}$$

Thus, the CDF of γ_1 expressed in (34) can be asymptotically rewritten as

$$F_{\gamma_1}(x) = \frac{\lambda_1^{k_1} x^{k_1}}{\Gamma(k_1) k_1 \bar{\gamma}_s^{k_1}} + o\left(\frac{x^{k_1+1}}{\bar{\gamma}_s^{k_1+1}}\right) \tag{19}$$

where $o(\cdot)$ stands for higher order terms. Combined with $F_{\gamma_2}(x)$ in (35), we have

$$F_{\gamma_{sd}}(x) = \frac{\Gamma(Lk_2+k_1)(\lambda_1\bar{\gamma}_I)^{k_1} x^{k_1}}{\Gamma(Lk_2)\Gamma(k_1)(\lambda_2\bar{\gamma}_s)^{k_1} k_1} + o\left(\bar{\gamma}_s^{-k_1-1}\right). \tag{20}$$

Then, substituting (20) into (9), $\mathcal{P}_{dire}$ can be obtained as

$$\mathcal{P}_{dire} = \frac{(2k_1-1)!!}{2} \frac{\Gamma(Lk_2+k_1)(\lambda_1\bar{\gamma}_I)^{k_1}}{\Gamma(Lk_2)\Gamma(k_1)(\lambda_2\bar{\gamma}_s\beta)^{k_1} k_1} \tag{21}$$

where $(n)!!$ is the double factorial notation [32, p. xliii].

2) Cooperative Mode: Firstly, we can obtain $f_{\gamma_{sd}}(x)$ by differentiating $F_{\gamma_{sd}}(x)$ as

$$f_{\gamma_{sd}}(x) = \frac{\Gamma(Lk_2+k_1)(\lambda_1\bar{\gamma}_I)^{k_1} x^{k_1-1}}{\Gamma(Lk_2)\Gamma(k_1)(\lambda_2\bar{\gamma}_s)^{k_1}} + o\left(\bar{\gamma}_s^{-k_1-1}\right). \tag{22}$$

Inserting (22) into (13), we can get

$$M_{\gamma_{sd}}(s) = \frac{\Gamma(Lk_2+k_1)(\lambda_1\bar{\gamma}_I)^{k_1} s^{-k_1}}{\Gamma(Lk_2)(\lambda_2\bar{\gamma}_s)^{k_1}} + o\left(\bar{\gamma}_s^{-k_1-1}\right). \tag{23}$$

To obtain $M_{\gamma_{srd}}(s)$, we need to derive $F_{\gamma_{srd}}$ firstly. Considering γ_{srd} specified in (7) is complex, to make the derivation of asymptotic $F_{\gamma_{srd}}$ tractable, we introduce the tight upper bound[4] as

$$\gamma_{srd} \le \gamma_{srd}^{up} = \min(U, V). \tag{24}$$

Then, the CDF of γ_{srd} can be written as

$$F_{\gamma_{srd}}(x) = 1 - [1 - F_U(x)][1 - F_V(x)]. \tag{25}$$

Define $P_r/P_s = \alpha$, i.e., $\bar{\gamma}_r = \alpha\bar{\gamma}_s$. Similar to the derivation of $F_{\gamma_{sd}}(x)$, $F_{\gamma_{srd}}(x)$ can be given by

$$F_{\gamma_{srd}}(x) = \begin{cases} \Phi_1\left(\frac{x}{\bar{\gamma}_s}\right)^{k_3} + o\left(\bar{\gamma}_s^{-k_3-1}\right), & k_3 < k_5 \\[2mm] \Phi_2\left(\frac{x}{\bar{\gamma}_s}\right)^{k_5} + o\left(\bar{\gamma}_s^{-k_5-1}\right), & k_3 > k_5 \\[2mm] \Phi_3\left(\frac{x}{\bar{\gamma}_s}\right)^{k} + o\left(\bar{\gamma}_s^{-k-1}\right), & k_3 = k_5 = k \end{cases} \tag{26}$$

where $\Phi_1 = \frac{\Gamma(Lk_4+k_3)(\lambda_3\bar{\gamma}_I)^{k_3}}{\Gamma(Lk_4)\Gamma(k_3)\lambda_4^{k_3} k_3}$, $\Phi_2 = \frac{\Gamma(Lk_2+k_5)(\lambda_5\bar{\gamma}_I)^{k_5}}{\Gamma(Lk_4)\Gamma(k_3)(\alpha\lambda_2)^{k_5} k_5}$, and $\Phi_3 = \Phi_1 + \Phi_2$. By substituting (26) into (43), we can get

$$M_{\gamma_{srd}}(s) = \begin{cases} \frac{\Phi_1\Gamma(k_3+1)}{\bar{\gamma}_s^{k_3}} s^{-k_3} + o\left(\bar{\gamma}_s^{-k_3-1}\right), & k_3 < k_5 \\[2mm] \frac{\Phi_2\Gamma(k_5+1)}{\bar{\gamma}_s^{k_5}} s^{-k_5} + o\left(\bar{\gamma}_s^{-k_5-1}\right), & k_3 > k_5 \\[2mm] \frac{\Phi_3\Gamma(k+1)}{\bar{\gamma}_s^{k}} s^{-k} + o\left(\bar{\gamma}_s^{-k-1}\right), & k_3 = k_5 = k. \end{cases} \tag{27}$$

Finally, inserting (23) and (27) into (17), we can finally get the asymptotic SER of the cooperative mode. As expected, we can observe that increasing the number of interferers L or the interfering power P_I ($P_I \propto \bar{\gamma}_I$) results in the increase of SER, which in turn deteriorates the system performance. Oppositely, increasing the transmit power at the satellite P_s ($P_s \propto \bar{\gamma}_s$) or the relay P_r ($P_r \propto \bar{\gamma}_r$) will improve the system performance.

IV. An Energy Efficient Adaptive Transmission Scheme

In the integrated satellite-terrestrial network where co-channel interference caused by resource reuse exists, cooperative transmission may not necessarily achieve higher transmission rate with various interfering scenarios

---

[4]Such an upper bound has been widely used in the literature for cooperative diversity systems [37].

and shadowing degrees. Moreover, in practice, the relay contributes to higher data-rate or more reliable transmission at the expense of not only extra transmit power consumption but also extra circuit power consumption. In this case, taking EE as the performance criteria is more attractive than considering transmission rate and power consumption individually. After obtaining SER expression as constraints, we focus on illustrating the proposed energy efficient adaptive transmission scheme in this section, where the trade-off among EE, SE, and SER are discussed. Moreover, ECE is evaluated as a complementary performance measure to SE and EE, offering an inherent tradeoff between SE and EE.

A. Spectral Efficiency and Energy Efficiency

Spectral efficiency (in bits/s/Hz) can be defined as the capacity of satellite communications, as given by

$$\eta_{SE} = \log_2(1 + \gamma_{end}) \tag{28}$$

where $\gamma_{end} = \gamma_{sd}$ in direct mode and $\gamma_{end} = \gamma_{coop}$ in cooperative mode.

Energy efficiency (in bits/Joule) is defined as the ratio of the system capacity (in bits/s) to the total power consumption (in Watt). For a given system bandwidth, B, the EE for the integrated satellite-terrestrial network can be mathematically expressed by

$$\eta_{EE}^m = \frac{B \cdot \eta_{SE}}{P_{total}}$$

$$= \begin{cases} \dfrac{\log_2(1 + \gamma_{sd})}{P_s^0 + P_c^s} & m = 0, \text{ if direct} \\ \dfrac{\frac{1}{2}\log_2(1 + \gamma_{coop})}{\frac{1}{2}\left(P_s^1 + P_r + P_c^s + P_c^r\right)} & m = 1, \text{ if coop} \end{cases} \tag{29}$$

where m represents the transmission mode. The direct mode and the cooperative mode are represented by $m = 0$ and $m = 1$, respectively. When measuring the total power consumption, we consider the operational power of the system which includes both the transmit power and the circuit power. Herein, P_s^0 and P_s^1 represent the transmit power of the satellite in direct and cooperative modes, respectively, P_c^s and P_c^r represent the circuit power of the satellite and the relay station, respectively. Note that the factor 1/2 in the cooperative mode indicates that the data received during the first phase and the second phase of the entire transmission are two copies of the same data sent from the satellite, which means one of them can be treated as redundant information in terms of transmission efficiency.

B. An Energy Efficient Adaptive Transmission Scheme With SER Constraints

In the following, we present an adaptive transmission scheme optimizing EE for the SER-constrained integrated satellite-terrestrial network. We select the transmission mode with higher EE while restrict the reliability of the satellite communication to an acceptable level, i.e., the SER is smaller

than the predefined threshold defined as $\mathcal{P}_{th}$. The optimization problem can be formulated as

$$\begin{aligned} \underset{(m, P_s^m)}{\text{maximize}} \quad & \eta_{EE}^m \\ \text{subject to} \quad & \mathcal{P}_m \leq \mathcal{P}_{th} \\ & P_s^0 = \frac{1}{2}\left(P_s^1 + P_r\right) \\ & P_s^m > 0. \end{aligned} \tag{30}$$

This optimization problem aims at illustrating the trade-off between EE and SER where both the efficiency and reliability are taken into account. As we all know, the SER constraint corresponds to a minimal transmit power constraint, which further affects the feasible region of SE. Thus, in the following, we will elaborate the effect of SER constraints on the optimal transmission mode from the perspective of EE-SE trade-off:

1) For each transmission mode, there is a trade-off between EE and SE, which means a maximum EE $\eta_{EE}^{\max}$ can be achieved with a certain SE, η_{SE}^*, $\eta_{SE}^* \in \left[0, \eta_{SE}^{\max}\right]$. When the network demands a desired reliability in data transmission (i.e., $\mathcal{P}_m \leq \mathcal{P}_{th}$), the region of the achievable SE is limited to a smaller range $\left[\eta_{SE}^{\min}, \eta_{SE}^{\max}\right]$, $\eta_{SE}^{\min} > 0$. In the integrated satellite-terrestrial network, two cases should be considered in terms of SER constraints and interfering scenarios. For a communication with relatively low reliability demands or in a mild interfering environment, we have $\eta_{SE}^{\min} \leq \eta_{SE}^*$. In this case, $\eta_{EE}^{\max}$ can also be achieved at point η_{SE}^*. However, for a communication with relatively high reliability demands or in a hostile interfering environment, we have $\eta_{SE}^{\min} > \eta_{SE}^*$. In this case, we can only achieve an optimal EE $\tilde{\eta}_{EE}$ at the point $\eta_{SE}^{\min}$, where $\tilde{\eta}_{EE} < \eta_{EE}^{\max}$.

2) Due to the fact that cooperative communication can benefit from the spatial diversity, the feasible SE of the direct transmission is limited to a smaller range compared with cooperative transmission under a certain SER constraint. However, the attainable EE of direct transmission may be superior to the cooperative ones', depending on the specific interfering scenario, which will be further illustrated in Section V.

In a word, we should choose the transmission mode according to the communication environment, such as different interfering scenarios, various shadowing degrees and so on, rather than adopting cooperative transmission aggressively.

By deriving the formulated problem, we can obtain the optimally energy efficient transmission mode and the corresponding transmit power. In the direct mode, we can adopt the conventional satellite design and there is no change to the satellite system. However, if the cooperative mode is adopted, some modifications are required at the satellite. For example, to realize the MRC at the destination user, accurate synchronization between the satellite and the terrestrial relay is needed. Moreover, when the optimal transmission mode is selected according to the proposed scheme in this paper, the satellite needs to inform the terrestrial terminals of the optimization results through control signals. Note that as our objective is to investigate a transmission scheme which can give consideration to both efficiency and reliability rather than implement the optimization algorithm, we perform an exhaustive search of the transmit power for the optimal value which maximize the EE.

TABLE I

SIMULATION PARAMETERS

Frequency	2 GHz (L/S band)
System bandwidth B	10 MHz
Transmit power of BS P_I	35 dBm
Circuit power of relay P_c^r	500 mW
Antenna gain of satellite	25 dBi
Satellite pathloss [43]	S-R,D 148dB
Terrestrial link pathloss model [38] (d in Km)	R-D $103.4 + 24.2\log_{10}(d)$ B-R $125.2 + 36.3\log_{10}(d)$ B-D $131.1 + 42.8\log_{10}(d)$
Noise power spectral density N_0	-174 dBm/Hz
Base service data rate R^{ref}	9.6 kbps
Revenue per bit k_r	6.94×10^{-6} dollars/bit
Energy cost per Joule k_c	2.8×10^{-4} dollars/J
Other cost per Joule C_0	5×10^{-3} dollars/s

C. Economic Efficiency

Inspired by [38] and [39], economic efficiency, measuring the profitability of the system (in monetary unit per second), is considered here as a complementary performance measure to SE and EE. ECE implicitly takes into account SE and EE as both metrics reflect revenues and costs of the system, therefore, it potentially offers a good trade-off between SE and EE, which can be sufficiently characterised by both η_{SE}^m and P^m.

Based on the observation in [40], a user is only willing to pay a small additive premium on top of the basic service for a multiplicative increase in the attainable data rate. Thus, the multifold increase in the achievable throughput bears only a marginal increase in the network's attainable revenue without the introduction of new services. This economic trend is known as the law of diminishing returns and leads to the attainable revenue being logarithmically proportional to the average data-rata attainable for each user. In this paper, by jointly considering η_{SE}^m and P^m, a generalized definition of ECE is given by

$$\eta_{ECE}^m = k_r R^{\text{ref}} \log_2\left(1 + \frac{B\eta_{SE}^m}{R^{\text{ref}}}\right) - \left(C_0 + k_c P^m\right) \quad (31)$$

where R^{ref} is the referenced service data rate which refers to the essential service expected by the mobile user. Here, k_r and k_c are the revenue per bit and energy cost per Joule (Watt-second), respectively, P^m is the total power consumption expended by the satellite and the relay station in the data transmission, and C_0 involves other costs (in monetary unit per second) in addition to the energy cost. Referred to [41] and [42], the value used for the ECE parameters in integrated satellite-terrestrial networks are shown in Table I.

V. RESULTS AND ANALYSIS

In this section, we take the low earth orbit (LEO) satellite communication scenario as an example to evaluate the proposed energy efficient adaptive transmission schemes. In this situation, the direct link from the satellite to the destination can be supported with the lower orbital altitude, e.g., 300 Km-800 Km. Here, L base stations regarded as interferers are uniformly distributed around the relay and

TABLE II

CHANNEL PARAMETERS [30]

Channel	Shadowing	σ	m_s	m_m	$\lambda = k$
Satellite links	ILS	0.161	38.0809	3	2.71
	AS	0.345	7.9115	2.5	1.73
	FHS	0.806	1.0931	2	0.53
Terrestrial links	R→D	0.806	1.0931	1.5	0.45
	BS$_i$→R	0.345	7.9115	2	1.45
	BS$_i$→D	0.806	1.0931	1.5	0.45

the destination. The interfering distance d_I is defined as the distance between the base stations and the midpoint of the relay-destination path. The simulation parameters are listed in Table I.

To characterize the shadowing and multipath fading environment in the integrated satellite-terrestrial network, satellite downlinks and terrestrial links are all modeled as generalized-K distributions with $\Omega_0 = 1$. The detailed channel parameters are given in Table II, where σ is the standard deviation of the log-normal shadowing and increases as the amount of fading increases. Using a moment matching technique [30], the corresponding parameter m_s of the generalized-K distribution can be linked to $m_s = \frac{1}{e^{\sigma^2}-1}$. In practical applications, the relay station is usually placed at a higher position than the destination user, which results in that S → D link usually experiences a more severe shadowing than S → R link. Thus, we consider two shadowing scenarios for the satellite downlinks in the integrated network. In the first scenario, S → R and S → D channels are assumed to experience infrequent light shadowing and average shadowing ($\sigma_{sr} = 0.161, \sigma_{sd} = 0.345$), referred to the ILS-AS scenario. In the second scenario, S → R and S → D channels are assumed to experience infrequent light shadowing and frequent heavy shadowing ($\sigma_{sr} = 0.161, \sigma_{sd} = 0.806$), referred to the ILS-FHS scenario. Compared with the satellite downlinks, terrestrial links with the same shadowing degree usually experience more severe multipath fading, which means smaller values for m_m as presented in Table II.

We first conduct numerical simulations to demonstrate the validity of the theoretical analysis and compare the SER performance of two transmission modes in the considered network, as shown in Fig. 2. Here, γ_{ave} denotes the average transmit SNR of one transmission, which corresponds to one phase in direct mode while two phases in cooperative mode. It can be observed that for both ILS-AS and ILS-FHS shadowing scenarios, the theoretical SER expressions are in excellent agreement with the simulation results, and the asymptotic results are tight in the high SNR region. As illustrated, in the given interfering environment, the SER performance of the cooperative mode outperforms the direct mode, demonstrating the benefits of the spatial diversity.

Fig. 3 shows the impact of the interferers' distribution on the SER performance of two transmission modes in the considered network. For small interfering distance, cooperative transmission has a worse SER performance than the direct transmission, which is due to the fact that the interference received in the S-R link is non-ignorable and amplified along
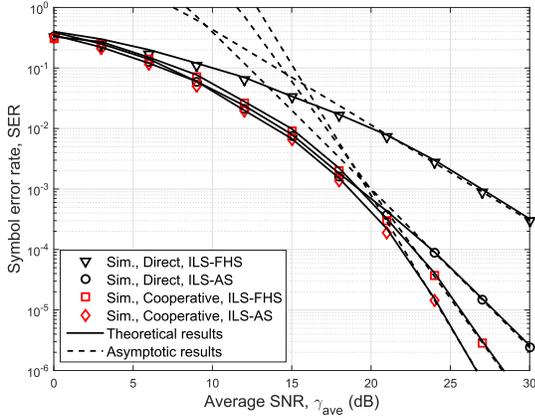
Fig. 2. Symbol error rate versus average SNR in ILS-AS and ILS-FHS shadowing scenarios ($d_I = 6$ Km, $L = 3$).
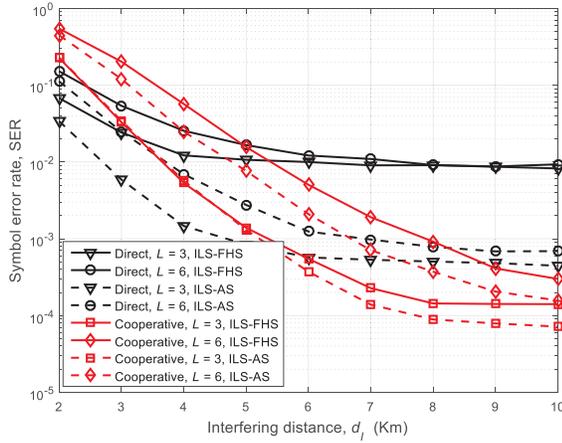
Fig. 3. Simulated symbol error rate versus d_I for different interferer numbers in ILS-AS and ILS-FHS shadowing scenarios ($\gamma_{ave} = 20$ dB).

Fig. 4. Energy efficiency versus average transmit power for three P_c^s cases in the ILS-FHS shadowing scenario ($d_I = 6$ Km, $L = 3$).
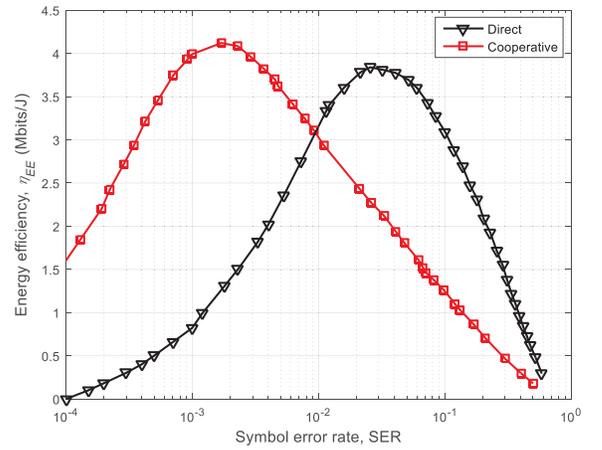
Fig. 5. Energy efficiency versus symbol error rate in the ILS-FHS shadowing scenario ($d_I = 6$ Km, $L = 3$, $P_c^s = 10$ W).

with signal by the AF-based relay node. Compared with the direct mode, an increase of the interfering distance causes a more noticeable improvement of the SER performance for cooperative transmission; Moreover, the SER gap between $L = 3$ and $L = 6$ becomes larger for the cooperative mode. Both phenomena indicate that cooperative transmission is more sensitive to the interference.

Then, we analyze EE of two transmission modes. Fig. 4 firstly depicts EE versus the average transmit power for three circuit power consumption P_c^s cases. It can be seen that for both transmission modes, when the circuit power increases which results in a larger power consumption, the achieved EE become smaller. Moreover, for each circuit power consumption case, as the transmit power increases, the EE of the cooperative mode outperforms the direct mode in the beginning and deteriorates afterwards. The reason behind is that when the transmit power is small, cooperative transmission can achieve much higher SE than the direct mode owing to its resistance to deep fading. While as the transmit power increases, the increase of the achievable SE cannot afford to the increase of the total power consumption. As a result, the superiority of cooperative mode vanishes and even obtains a worse EE performance than the direct mode. It is interesting to note that the optimal

average transmit power is increasing in the circuit power consumption. For example, in cooperative mode, the optimal transmit power is 1.5 dBW as $P_c^s = 8$ W and while increases to 3 dBW as $P_c^s = 12$ W. This phenomenon implies that when circuit power consumption increases, we need to increase transmit power rather than decreasing it to achieve higher EE, although the total power consumption will increase.

Fig. 5 depicts EE versus SER. From the figure we can see there is a trade-off between the efficiency and the quality of service (QoS). When the network demands relatively high reliability in data transmission (i.e., $\mathcal{P}_{th}$ is small), the cooperative mode achieves considerably larger EE than the direct mode, while lower EE when SER is large. This phenomenon can be explained by integrating two facts into account. One is that direct transmission requires more transmit power than the cooperative transmission for a desired SER shown in Fig. 2, and the other is the EE trends versus transmit power shown in Fig. 4.

Fig. 6 presents EE versus SE with different interfering distance. For the same SE, the relation of EE for two transmission modes can be obtained by comparing the total power consumption. Since the circuit power is the main constituent in the power consumption at low SE region, cooperative
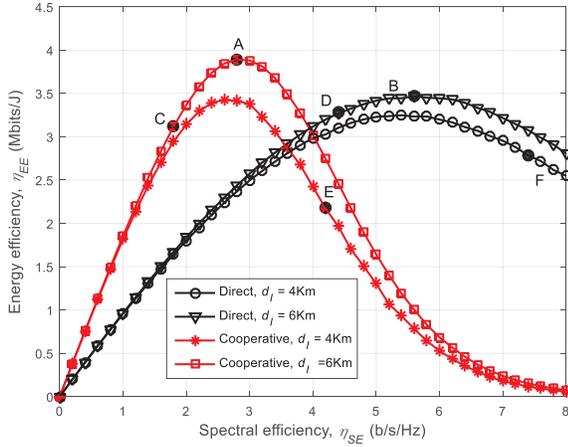
Fig. 6. Energy efficiency versus spectral efficiency in the ILS-FHS shadowing scenario ($\mathcal{P}_{th} = 10^{-3}$, $L = 3$, $P_c^s = 10$ W).

Fig. 7. Energy efficiency versus interfering distance d_I in the ILS-FHS shadowing scenario ($\mathcal{P}_{th} = 10^{-3}$, $\gamma_{ave} = 20$ dB, $P_c^s = 10$ W).

mode can achieve higher EE with lower average circuit power $\left(\frac{1}{2}\left(P_c^s + P_c^r\right) \ll P_c^s\right)$. On the other hand, due to the redundant transmission in the second phase, the average transmit power of cooperative mode is much higher than the direct ones' as SE increases, resulting in a lower EE at high SE region. Moreover, the trade-off between EE and SE is also shown as we explained before. Specifically, for cooperative transmission, the points on the curve before point A are seen to be non-optimal as they are always worse than point A in terms of both EE and SE. Analogously, the optimal frontier for direct transmission are indicated with point B. Furthermore, the maximum EE of cooperative transmission is larger than the maximum EE of direct transmission. It can also be observed that when there is a certain SER constraint, the feasible SE of the direct transmission is limited to a smaller range compared with cooperative transmission, i.e., [C, SE_{max}] and [D, SE_{max}] for $d_I = 6$ Km; [E, SE_{max}] and [F, SE_{max}] for $d_I = 4$ Km. Nevertheless, within its feasible SE region, direct transmission is shown to potentially achieve better EE than cooperative transmission when the interfering distance is small.

We compare EE of the direct mode and the cooperative mode for ILS-FHS and ILS-AS shadowing scenarios in Fig. 7 and Fig. 8, respectively, illustrating which transmission mode is more efficient for a specific interfering scenario, i.e., given interfering distance and the number of interferers. For the ILS-FHS scenario, when $L = 3$, the intersection of two transmission modes appears in 4.7 Km. In this case, from the perspective of EE, we should choose direct mode if the interfering distance is less than 4.7 Km. When $L = 6$, the intersection moves right to about 5.5 Km, which implies that direct mode outperforms cooperative mode in sever interference scenario. For the ILS-AS scenario, the intersections all move towards long interfering distance. Besides, comparison of two figures indicates that direct mode is more sensitive to the fading condition, while cooperative mode is more sensitive to the interference.

To further illustrate the advantage of the adaptive transmission scheme proposed in this paper, we compare the EE of the adaptive transmission with direct transmission and cooperative transmission in Fig. 9. From the figure we can see that, EE of
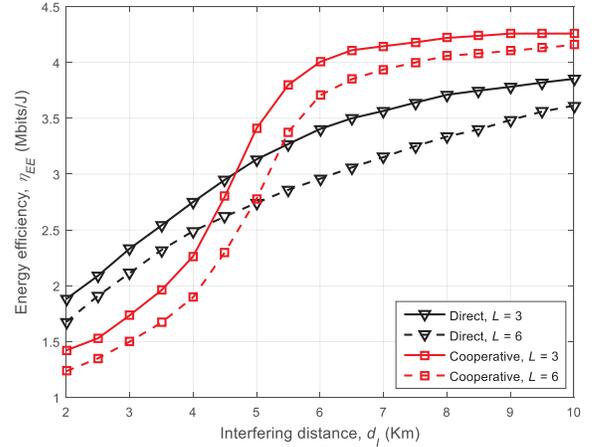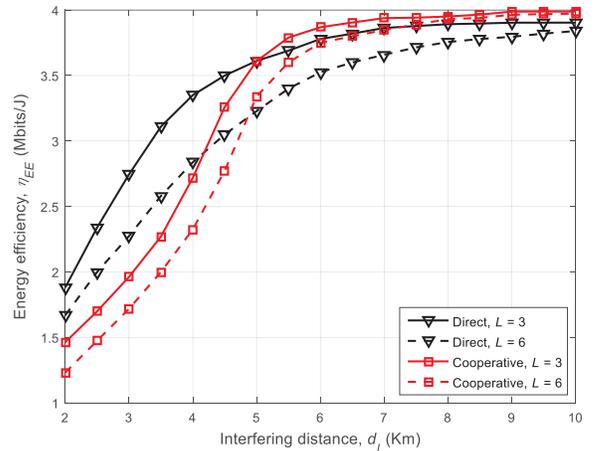
Fig. 8. Energy efficiency versus interfering distance d_I in the ILS-AS shadowing scenario ($\mathcal{P}_{th} = 10^{-3}$, $\gamma_{ave} = 20$ dB, $P_c^s = 10$ W).
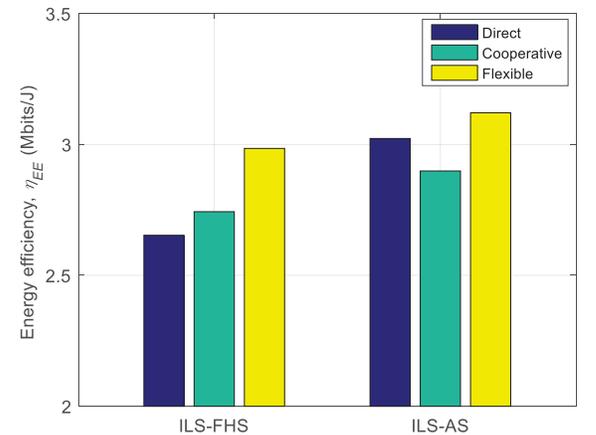
Fig. 9. Energy efficiency comparison among three transmission schemes ($\mathcal{P}_{th} = 10^{-3}$, $\gamma_{ave} = 20$ dB, $P_c^s = 10$ W).

the adaptive scheme is about 13% and 11% higher than the direct one and the cooperative one in the ILS-FHS scenario, respectively, while 5% and 10% in the ILS-AS scenario. The results indicate that we should choose the transmission mode according to specific interfering scenarios and shadowing degrees, rather than adopting cooperative transmission aggressively.
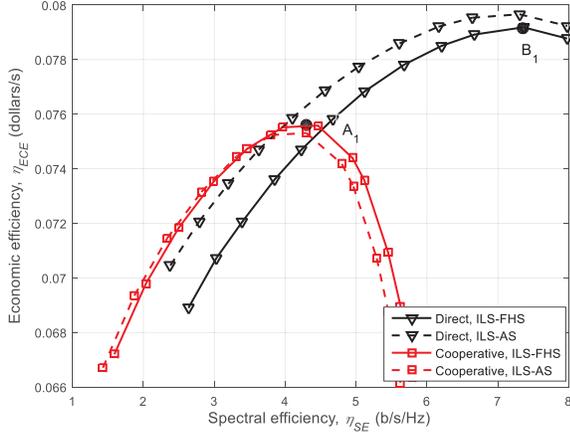
Fig. 10. Economic efficiency versus spectral efficiency ($d_I = 6$ Km, $L = 3$, $P_c^s = 10$ W).
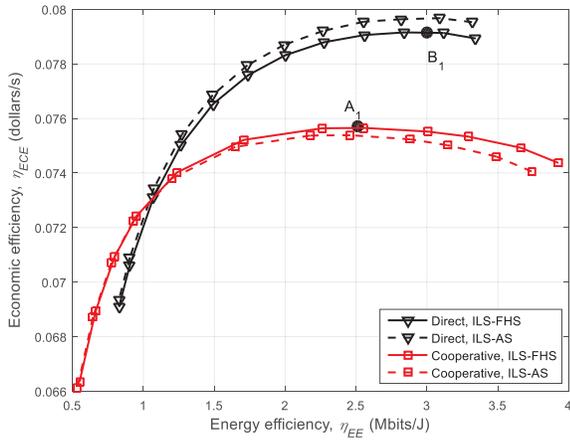
Fig. 11. Economic efficiency versus energy efficiency ($d_I = 6$ Km, $L = 3$, $P_c^s = 10$ W).

We illustrated the trade-off between EE and SE before, and we know the optimal frontiers represent efficient operating points, such that an extra advantage of one performance metric can only be achieved by trading it off with the benefits of other metric. A sensible operating point on the optimal frontiers can be obtained by evaluating a complementary metric, such as ECE, along the trade-off curves as illustrated in Fig. 10 and Fig. 11. From the figures we can see that, the strategy for maximizing ECE is to operate at points A_1 and B_1 for cooperative and direct transmissions, respectively, rather than operating at the optimal frontiers represented by A and B in Fig. 6. These results show that considering revenue and cost in practical application, ECE provides a balanced direction in designing the transmission parameters.

VI. CONCLUSIONS

In this paper, an energy efficient adaptive transmission scheme for the integrated satellite-terrestrial network with SER constraints has been proposed. In a composite multipath/ shadowing fading environment, theoretical analyses on the SER performance of two transmission modes have been conducted and close approximations in comparison with simulation results have been achieved. Based on the closed-form expressions, fundamental trade-offs among SE, SER, and EE have been investigated. numerical results have shown that compared with the cooperative transmission, the feasible SE of the direct transmission is limited to a smaller range under a certain SER requirement. However, within its feasible SE region, direct transmission tends to achieve better EE than cooperative transmission when the interfering distance is small, which indicates that the transmission mode should be adopted adaptively according to different interfering scenarios and shadowing degrees. The performance of ECE has also been analyzed and it has shown that ECE can serve as a complementary performance metric for EE and SE trade-off.

APPENDIX A
DERIVATION OF SER IN DIRECT TRANSMISSION

A. Derivation of $F_{\gamma_{sd}}(x)$

From the expression of γ_{sd} in (2), $F_{\gamma_{sd}}(x)$ can be calculated as

$$F_{\gamma_{sd}}(x) = \int_0^\infty F_{\gamma_1}[x(y+1)] f_{\gamma_2}(y) dy. \quad (32)$$

To make the derivation tractable, we rewrite the PDF of generalized-K model into a Gamma distributed format with a shape parameter k and a scale parameter λ, where $k = \frac{m_m m_s}{m_m + m_s + 1}$ and $\lambda = k/\Omega_0$ [33], i.e.,

$$f_{\gamma_1}(x) = \frac{\lambda_1^{k_1}}{\Gamma(k_1) \bar{\gamma}_s^{k_1}} x^{k_1-1} e^{-\frac{\lambda_1}{\bar{\gamma}_s} x}, \quad x > 0. \quad (33)$$

Then, using [32, eqs. (3.351.1) and (8.352.1)], we obtain

$$F_{\gamma_1}(x) = \frac{\Upsilon\left(k_1, \frac{\lambda_1}{\bar{\gamma}_s} x\right)}{\Gamma(k_1)} = 1 - \sum_{m=0}^{k_1-1} \frac{\lambda_1^m x^m e^{-\frac{\lambda_1}{\bar{\gamma}_s} x}}{m! \bar{\gamma}_s^m} \quad (34)$$

where $\Upsilon(\alpha, x) = \int_0^x e^{-t} t^{\alpha-1} dt$ denotes the lower incomplete Gamma function [32, eq. (8.350.1)].

Recall that $\gamma_2 = \bar{\gamma}_I \sum_{i=1}^{i=L} |h_{id}|^2$. From [33] we know that, the PDF of the sum of L independent generalized-K random variables can be approximated by a Gamma distribution with a shape parameter Lk and a scale parameter λ, i.e.,

$$f_{\gamma_2}(x) = \frac{\lambda_2^{Lk_2}}{\Gamma(Lk_2) \bar{\gamma}_I^{Lk_2}} x^{Lk_2-1} e^{-\frac{\lambda_2}{\bar{\gamma}_I} x}, \quad x > 0. \quad (35)$$

By substituting (34) and (35) into (32), and carrying out some mathematical manipulation, we obtain $F_{\gamma_{sd}}(x)$ as

$$F_{\gamma_{sd}}(x) = 1 - \sum_{m=0}^{k_1-1} \frac{\lambda_1^m \lambda_2^{Lk_2} x^m e^{-\frac{\lambda_1}{\bar{\gamma}_s} x}}{m! \Gamma(Lk_2) \bar{\gamma}_s^m \bar{\gamma}_I^{Lk_2}}$$
$$\times \int_0^\infty y^{Lk_2-1} (y+1)^m e^{-\left(\frac{\lambda_2}{\bar{\gamma}_I} + \frac{\lambda_1}{\bar{\gamma}_s} x\right) y} dy. \quad (36)$$

Finally, using the Binomial theorem and employing [32, eq. (3.351.3)], we obtain the desired CDF of γ_{sd} shown in (10).

B. Derivation of $\mathcal{P}_{Dire}$

By substituting (10) into (9), we rewrite $\mathcal{P}_{dire}$ as

$$
\mathcal{P}_{dire} = \frac{\sqrt{2}}{4\sqrt{\pi}} \int_0^\infty \frac{e^{-\frac{y}{2}}}{\sqrt{y}} dy - \frac{\sqrt{2}}{4\sqrt{\pi}}
$$
$$
\times \sum_{m=0}^{k_1-1} \frac{\lambda_1^m \lambda_2^{Lk_2} \beta^{-m}}{m! \bar{\gamma}_s^m \bar{\gamma}_I^{Lk_2}} \sum_{q=0}^{m} \binom{m}{q} (Lk_2)_q \mathcal{I}_1 \qquad (37)
$$

where

$$
\mathcal{I}_1 = \int_0^\infty y^{m-\frac{1}{2}} e^{-\left(\frac{\lambda_1}{\bar{\gamma}_s\beta}+\frac{1}{2}\right)y} \left(\frac{\lambda_2}{\bar{\gamma}_I} + \frac{\lambda_1}{\bar{\gamma}_s\beta} y\right)^{-Lk_2-q} dy. \qquad (38)
$$

To solve this integral, we first express $\left(\frac{\lambda_2}{\bar{\gamma}_I} + \frac{\lambda_1 y}{\bar{\gamma}_s\beta}\right)^{-Lk_2-q}$ in terms of Meijer-G function as [34, eq. (10)] as

$$
\left(\frac{\lambda_2}{\bar{\gamma}_I} + \frac{\lambda_1 y}{\bar{\gamma}_s\beta}\right)^{-Lk_2-q}
$$
$$
= \frac{(\bar{\gamma}_I/\lambda_2)^{Lk_2+q}}{\Gamma(Lk_2+q)} G_{11}^{11}\left[\frac{\lambda_1\bar{\gamma}_I y}{\lambda_2\bar{\gamma}_s\beta} \middle| \begin{matrix} 1-Lk_2-q \\ 0 \end{matrix}\right]. \qquad (39)
$$

Then, with the aid of [32, eqs. (7.813.1) and (9.31.2)], $\mathcal{P}_{dire}$ can be obtained as in (11).

APPENDIX B
DERIVATION OF SER IN COOPERATIVE TRANSMISSION

A. Derivation of M_{sd}

To obtain M_{sd}, we need to derive $f_{\gamma_{sd}}(x)$ first, which can be calculated as

$$
f_{\gamma_{sd}}(x) = \int_0^\infty (y+1) f_{\gamma_2}(y) f_{\gamma_1}[x(y+1)] dy. \qquad (40)
$$

After substituting the required PDFs and using the Binomial theorem, we obtain

$$
f_{\gamma_{sd}}(x) = \frac{\lambda_1^{k_1} \lambda_2^{Lk_2}}{\Gamma(k_1) \bar{\gamma}_s^{k_1} \bar{\gamma}_I^{Lk_2}} \sum_{h=0}^{k_1} \binom{k_1}{h} (Lk_2)_h x^{k_1-1}
$$
$$
\times e^{-\frac{\lambda_1}{\bar{\gamma}_s}x} \left(\frac{\lambda_2}{\bar{\gamma}_I} + \frac{\lambda_1}{\bar{\gamma}_s}x\right)^{-Lk_2-h}. \qquad (41)
$$

Then, substituting (41) into (13) and simplifying, $M_{\gamma_{sd}}(s)$ can be given by

$$
M_{\gamma_{sd}}(s) = \frac{\lambda_1^{k_1} \lambda_2^{Lk_2}}{\Gamma(k_1) \bar{\gamma}_s^{k_1} \bar{\gamma}_I^{Lk_2}} \sum_{h=0}^{k_1} \binom{k_1}{h} (Lk_2)_h
$$
$$
\times \int_0^\infty x^{k_1-1} e^{-\left(s+\frac{\lambda_1}{\bar{\gamma}_s}\right)x} \left(\frac{\lambda_2}{\bar{\gamma}_I} + \frac{\lambda_1}{\bar{\gamma}_s}x\right)^{-Lk_2-h} dx. \qquad (42)
$$

Similar to the derivation of $\mathcal{I}_1$, the analytical expression for $M_{\gamma_{sd}}(s)$ can be obtained as (15).

B. Derivation of M_{srd}

Due to the fact that a closed-form expression for the PDF of γ_{srd} specified in (7) is mathematically intractable, we employ the CDF based MGF method through integration by parts of (13), i.e.,

$$
M_{\gamma_{srd}}(s) = \int_0^\infty s e^{-s\gamma} F_{\gamma_{srd}}(\gamma) d\gamma. \qquad (43)
$$

Form (7), $F_{\gamma_{srd}}$ can be calculated as

$$
F_{\gamma_{srd}}(x) = \Pr\left(\frac{UV}{U+V+1} < x\right)
$$
$$
= \int_0^x \Pr\left(U > \frac{x(y+1)}{y-x}\right) f_V(y) dy
$$
$$
+ \int_x^\infty \Pr\left(U \le \frac{x(y+1)}{y-x}\right) f_V(y) dy
$$
$$
= \int_0^x f_V(y) dy + \int_x^\infty F_U\left(\frac{x(y+1)}{y-x}\right) f_V(y) dy. \qquad (44)
$$

In cooperative communications, both the relay and the destination will be corrupted by the interference. In this case, we assume the interference dominates the noise. By changing the variable as $z = y - x$, we obtain

$$
F_{\gamma_{srd}}(x) = 1 - \int_0^\infty \left[1 - F_U\left(\frac{x(x+z)}{z}\right)\right] f_V(x+z) dz \qquad (45)
$$

where $F_U(x)$ can be expressed as

$$
F_U(x) = 1 - \sum_{n=0}^{k_3-1} \frac{\lambda_3^n \lambda_4^{Lk_4} x^n e^{-\frac{\lambda_3}{\bar{\gamma}_s}x}}{n! \Gamma(Lk_4) \bar{\gamma}_s^n \bar{\gamma}_I^{Lk_4}}
$$
$$
\times \int_0^\infty y^{Lk_4-1}(y+1)^n e^{-\frac{\lambda_4}{\bar{\gamma}_I}y} e^{-\frac{\lambda_3}{\bar{\gamma}_s}xy} dy. \qquad (46)
$$

Here, expressing $e^{-\frac{\lambda_4}{\bar{\gamma}_I}y}$ into series with N terms and employing [32, eq. (3.351.3)], yields

$$
F_U(x) = 1 - \sum_{n=0}^{k_3-1} \frac{\lambda_3^n}{n!\bar{\gamma}_s^n} \sum_{l=0}^{N} \frac{(-1)^l}{l!} \left(\frac{\lambda_4\bar{\gamma}_s}{\lambda_3\bar{\gamma}_I}\right)^{Lk_4+l}
$$
$$
\times \sum_{p=0}^{n} \binom{n}{p} (Lk_4)_{l+p} \frac{\bar{\gamma}_s^p}{\lambda_3^p} x^{-\tilde{p}} e^{-\frac{\lambda_3}{\bar{\gamma}_s}x} \qquad (47)
$$

where $\tilde{p} = Lk_4 + l + p - n$. Similarly, $f_V(x)$ can be written as $f_V(x) = \int_0^\infty y f_{\gamma_2}(y) f_{\gamma_5}(xy) dy$ and obtained as

$$
f_V(x) = \left(\frac{\lambda_2\bar{\gamma}_r}{\lambda_5\bar{\gamma}_I}\right)^{Lk_2} \frac{(Lk_2)_{k_5}}{\Gamma(k_5)} x^{-Lk_2-1}. \qquad (48)
$$

By substituting (47) and (48) into (45), we can get

$$
F_{\gamma_{srd}}(x) = 1 - \sum_{n=0}^{k_3-1} \frac{\lambda_3^n}{n!\bar{\gamma}_s^n} \sum_{l=0}^{N} \frac{(-1)^l}{l!} \left(\frac{\lambda_4\bar{\gamma}_s}{\lambda_3\bar{\gamma}_I}\right)^{Lk_4+l} \sum_{p=0}^{n} \binom{n}{p}
$$
$$
\times (Lk_4)_{l+p} \frac{\bar{\gamma}_s^p}{\lambda_3^p} \left(\frac{\lambda_2\bar{\gamma}_r}{\lambda_5\bar{\gamma}_I}\right)^{Lk_2} \frac{(Lk_2)_{k_5}}{\Gamma(k_5)} x^{-\tilde{p}} \mathcal{I}_2 \qquad (49)
$$

where

$$\mathcal{I}_2 = \int_0^\infty \frac{z^{\tilde{p}}}{(x+z)^{\tilde{p}+Lk_2+1}} e^{-\frac{\lambda_3 x^2}{\bar{\gamma}_s z}} \, dz. \qquad (50)$$

To solve the integral, we express $e^{-\frac{\lambda_3 x^2}{\bar{\gamma}_s z}}$ in terms of Meijer-G function with [34, eq. (11)] and [32, eq. (9.31.2)], i.e.,

$$e^{-\frac{\lambda_3 x^2}{\bar{\gamma}_s z}} = G_{01}^{10}\left[\frac{\lambda_3 x^2}{\bar{\gamma}_s z}\middle| \begin{array}{c} - \\ 0 \end{array}\right] = G_{10}^{01}\left[\frac{\bar{\gamma}_s}{\lambda_3 x^2} z\middle| \begin{array}{c} 1 \\ - \end{array}\right]. \qquad (51)$$

Then, using [35, eq. (07.34.21.0086.01)], we further obtain

$$\mathcal{I}_2 = \frac{x^{-Lk_2}}{\Gamma(\tilde{p}+Lk_2+1)} G_{12}^{21}\left[\frac{\lambda_3 x}{\bar{\gamma}_s}\middle| \begin{array}{c} 1-Lk_2 \\ 1+\tilde{p}, 0 \end{array}\right]. \qquad (52)$$

By substituting $F_{\gamma_{srd}}(x)$ into (43) and proceeding, we can get

$$M_{\gamma_{srd}}(x) = 1 - \sum_{n=0}^{k_3-1} \frac{\lambda_3^n}{n!\bar{\gamma}_s^n} \sum_{l=0}^{N} \frac{(-1)^l}{l!} \left(\frac{\lambda_4 \bar{\gamma}_s}{\lambda_3 \bar{\gamma}_I}\right)^{Lk_4+l} \sum_{p=0}^{n} \binom{n}{p}$$
$$\times \frac{\bar{\gamma}_s^p}{\lambda_3^p} \left(\frac{\lambda_2 \bar{\gamma}_r}{\lambda_5 \bar{\gamma}_I}\right)^{Lk_2} \frac{(Lk_2)_{k_5}}{\Gamma(k_5)} \frac{(Lk_4)_{l+p}}{\Gamma(\tilde{p}+Lk_2+1)} \mathcal{I}_3 \qquad (53)$$

where

$$\mathcal{I}_3 = \int_0^\infty s e^{-sx} x^{-\tilde{p}-Lk_2} G_{12}^{21}\left[\frac{\lambda_3 x}{\bar{\gamma}_s}\middle| \begin{array}{c} 1-Lk_2 \\ 1+\tilde{p}, 0 \end{array}\right] dx. \qquad (54)$$

Using [32, eq. (7.813.1)], $\mathcal{I}_3$ can be derived as

$$\mathcal{I}_3 = s^{\tilde{p}+Lk_2} G_{22}^{22}\left[\frac{\bar{\gamma}_s s}{\lambda_3}\middle| \begin{array}{c} -\tilde{p}, 1 \\ 1-\tilde{p}-Lk_2, Lk_2 \end{array}\right]. \qquad (55)$$

Until now, closed-form expressions for $M_{\gamma_{sd}}$ and $M_{\gamma_{srd}}$ have all been obtained.

REFERENCES

[1] P.-D. Arapoglou, K. Liolis, M. Bertinelli, A. Panagopoulos, P. Cottis, and R. de Gaudenzi, "MIMO over satellite: A review," *IEEE Commun. Surveys Tuts.*, vol. 13, no. 1, pp. 27–51, 1st Quart., 2011.

[2] J. P. Choi and C. Joo, "Challenges for efficient and seamless space-terrestrial heterogeneous networks," *IEEE Commun. Mag.*, vol. 53, no. 5, pp. 156–162, May 2015.

[3] Y. Labrador, M. Karimi, D. Pan, and J. Miller, "An approach to cooperative satellite communications in 4G mobile systems," *J. Commun.*, vol. 4, no. 10, pp. 815–826, Nov. 2009.

[4] B. Paillassa, B. Escrig, R. Dhaou, M.-L. Boucheret, and C. Bes, "Improving satellite services with cooperative communications," *Int. J. Satellite Commun.*, vol. 29, no. 6, pp. 479–500, Oct. 2011.

[5] M. R. Bhatnagar and M. K. Arti, "Performance analysis of AF based hybrid satellite-terrestrial cooperative network over generalized fading channels," *IEEE Commun. Lett.*, vol. 17, no. 10, pp. 1912–1915, Oct. 2013.

[6] Y. Ruan, Y. Li, R. Zhang, and H. Zhang, "Performance analysis of hybrid satellite-terrestrial cooperative networks with distributed alamouti code," in *Proc. IEEE VTC Spring*, Nanjing, China, May 2016, pp. 1–5.

[7] M. K. Arti and S. K. Jindal, "OSTBC transmission in shadowed-Rician land mobile satellite links," *IEEE Trans. Veh. Technol.*, vol. 65, no. 7, pp. 5771–5777, Jul. 2016.

[8] M. K. Arti and M. R. Bhatnagar, "Beamforming and combining in hybrid satellite-terrestrial cooperative systems," *IEEE Commun. Lett.*, vol. 18, no. 3, pp. 483–486, Mar. 2014.

[9] S. Sreng, B. Escrig, and M.-L. Boucheret, "Exact outage probability of a hybrid satellite terrestrial cooperative system with best relay selection," in *Proc. IEEE ICC*, Budapest, Hungary, Jul. 2013, pp. 4520–4524.

[10] P. K. Upadhyay and P. K. Sharma, "Max-max user-relay selection scheme in multiuser and multirelay hybrid satellite-terrestrial relay systems," *IEEE Commun. Lett.*, vol. 20, no. 2, pp. 268–271, Feb. 2016.

[11] B. Evans, M. Werner, E. Lutz, M. Bousquet, G. E. Corazza, and G. Maral, "Integration of satellite and terrestrial systems in future multimedia communications," *IEEE Wireless Commun.*, vol. 12, no. 5, pp. 72–80, Oct. 2005.

[12] M. Sadek and S. Aissa, "Personal satellite communication: Technologies and challenges," *IEEE Wireless Commun.*, vol. 19, no. 6, pp. 28–35, Dec. 2012.

[13] V. Deslandes, J. Tronc, and A. L. Beylot, "Analysis of interference issues in integrated satellite and terrestrial mobile systems," in *Proc. IEEE ASMA/SPSC*, Cagliari, Italy, Sep. 2010, pp. 256–261.

[14] X. Zhu, R. Shi, W. Feng, N. Ge, and J. Lu, "Position-assisted interference coordination for integrated terrestrial-satellite networks," in *Proc. IEEE PIMRC*, Hong Kong, Sep. 2015, pp. 971–975.

[15] U. Park, H. W. Kim, D. S. Oh, and D.-I. Chang, "Performance analysis of dynamic resource allocation for interference mitigation in integrated satellite and terrestrial systems," in *Proc. 9th Int. Conf. Next Generat. Mobile Appl., Serv. Technol.*, Cambridge, U.K., Sep. 2015, pp. 217–221.

[16] K. An *et al.*, "Performance analysis of multi-antenna hybrid satellite-terrestrial relay networks in the presence of interference," *IEEE Trans. Commun.*, vol. 63, no. 11, pp. 4390–4404, Nov. 2015.

[17] L. Yang and M. O. Hasna, "Performance analysis of amplify-and-forward hybrid satellite-terrestrial networks with cochannel interference," *IEEE Trans. Commun.*, vol. 63, no. 12, pp. 5052–5061, Dec. 2015.

[18] S. M. R. Bhavani, S. Maleki, G. Zheng, A. Awoseyila, B. Evans, and B. Ottersten, "GEO satellite feeder links and terrestrial full-duplex small cells: A case for coexistence," in *Proc. IEEE VTC-Spring*, Nanjing, China, May 2016, pp. 1–5.

[19] M. Höyhtyä, "Sharing FSS satellite C band with secondary small cells and D2D communications," in *Proc. IEEE ICC*, London, U.K., Jun. 2015, pp. 1606–1611.

[20] I. Ku, C.-X. Wang, and J. Thompson, "Spectral-energy efficiency trade-off in relay-aided cellular networks," *IEEE Trans. Wireless Commun.*, vol. 12, no. 10, pp. 4970–4982, Oct. 2013.

[21] Y. Xu, Y. Wang, R. Sun, and Y. Zhang, "Joint relay selection and power allocation for maximum energy efficiency in hybrid satellite-aerial-terrestrial systems," in *Proc. IEEE PIMRC*, Valencia, Spain, Sep. 2016, pp. 1–6.

[22] Y. Ruan, Y. Li, C.-X. Wang, R. Zhang, and H. Zhang, "Outage performance of integrated satellite-terrestrial networks with hybrid CCI," *IEEE Commun. Lett.*, vol. 21, no. 7, pp. 1545–1548, Jul. 2017.

[23] G. N. Kamga, M. Xia, and S. Aïssa, "A unified performance evaluation of integrated mobile satellite systems with ancillary terrestrial component," in *Proc. IEEE ICC*, London, U.K., Jul. 2015, pp. 934–938.

[24] S. Kim, "Evaluation of cooperative techniques for hybrid/integrated satellite systems," in *Proc. IEEE ICC*, Kyoto, Japan, Jul. 2011, pp. 1–5.

[25] B. Evans, O. Onireti, T. Spathopoulos, and M. A. Imran, "The role of satellites in 5G," in *Proc. EUSIPCO*, Nice, France, Sep. 2015, pp. 2756–2760.

[26] F. Alagoz and G. Gur, "Energy efficiency and satellite networking: A holistic overview," *Proc. IEEE*, vol. 99, no. 11, pp. 1954–1979, Nov. 2011.

[27] M. K. Arti, "Channel estimation and detection in hybrid satellite–terrestrial communication systems," *IEEE Trans. Veh. Technol.*, vol. 65, no. 7, pp. 5764–5771, Jul. 2016.

[28] C. Loo, "A statistical model for a land mobile satellite link," *IEEE Trans. Veh. Technol.*, vol. 34, no. 3, pp. 122–127, Aug. 1985.

[29] A. Abdi, W. C. Lau, M.-S. Alouini, and M. Kaveh, "A new simple model for land mobile satellite channels: First- and second-order statistics," *IEEE Trans. Wireless Commun.*, vol. 2, no. 3, pp. 519–528, May 2003.

[30] K. P. Peppas, "Accurate closed-form approximations to generalised-K sum distributions and applications in the performance analysis of equal-gain combining receivers," *IET Commun.*, vol. 5, no. 7, pp. 982–989, May 2011.

[31] M. K. Simon and M. S. Alouini, *Digital Communication Over Fading Channels*. Hoboken, NJ, USA: Wiley, 2005.

[32] I. S. Gradshteyn and I. M. Ryzhik, *Table of Integrals, Series, and Products*, 6th ed. San Francisco, CA, USA: Academic, 2000.

[33] S. Al-Ahmadi and H. Yanikomeroglu, "On the approximation of the generalized-K distribution by a gamma distribution for modeling composite fading channels," *IEEE Trans. Wireless Commun.*, vol. 9, no. 2, pp. 706–713, Feb. 2010.

[34] V. S. Adamchik and O. I. Marichev, "The algorithm for calculating integrals of hypergeometric type functions and its realization in REDUCE system," in *Proc. Int. Conf. Symp. Algebraic Comput.*, 1990, pp. 212–224.

[35] [Online]. Available: http://function.wolfram.com/07.34.21.0086.01

[36] M. R. Mckay, A. Zanella, I. B. Collings, and M. Chiani, "Error probability and SINR analysis of optimum combining in rician fading," *IEEE Trans. Commun.*, vol. 57, no. 3, pp. 676–687, Mar. 2009.

[37] S. S. Ikki and S. Aissa, "Performance analysis of two-way amplify-and-forward relaying in the presence of co-channel interferences," *IEEE Trans. Commun.*, vol. 60, no. 4, pp. 933–939, Apr. 2012.

[38] I. Ku, C.-X. Wang, and J. Thompson, "Spectral, energy and economic efficiency of relay-aided cellular networks," *IET Commun.*, vol. 7, no. 14, pp. 1476–1486, Sep. 2013.

[39] P. Patcharamaneepakorn *et al.*, "Spectral, energy, and economic efficiency of 5G multicell massive MIMO systems with generalized spatial modulation," *IEEE Trans. Veh. Technol.*, vol. 65, no. 12, pp. 9715–9731, Dec. 2016.

[40] J. Akhtman and L. Hanzo, "Power versus bandwidth-efficiency in wireless communications: The economic perspective," in *Proc. IEEE VTC-Fall*, Anchorage, AK, USA, Sep. 2009, pp. 1–5.

[41] *State of the Satellite Industry Report*, Satellite Industry Association, Washington, DC, USA, Jun. 2016.

[42] M. Richharia, *Mobile Satellite Communications: Principles and Trends*. Hoboken, NJ, USA: Wiley, 2014.

[43] S. Cakaj, B. Kamo, A. Lala, and A. Rakipi, "Elevation impact on signal to spectral noise density ratio for Low Earth Orbiting satellite ground station at S-band," in *Proc. Sci. Inf. Conf.*, London, U.K., Aug. 2014, pp. 641–645.

Yuhan Ruan received the B.S. degree in telecommunications engineering from Xidian University, Xi'an, China, in 2013. She is currently pursuing the Ph.D. degree in communication and information system with Xidian University. She was a visiting Ph.D. student under the supervision of Professor C.-X. Wang with Heriot-Watt University, Edinburgh, U.K., from 2016 to 2017. Her current research interests are in the fields of satellite-terrestrial networks, cooperative communications, cognitive radio techniques, and energy efficient wireless networks.

Yongzhao Li (M'04–SM'17) received the B.S., M.S., and Ph.D. degrees in electronic engineering from Xidian University, Xi'an, China, in 1996, 2001, and 2005, respectively. Since 1996, he has been with Xidian University, where he is currently a Full Professor with the State Key Laboratory of Integrated Services Networks, Xidian University. He was a Research Professor with the University of Delaware, Newark, DE, USA, from 2007 to 2008, and the University of Bristol, Bristol, U.K., in 2011, respectively. In 2008, he received the Best Paper Award of the IEEE ChinaCOM'08 international conference. Due to his excellent contributions in education and research, in 2012, he received the Program for New Century Excellent Talents in University, Ministry of Education, China. He also serves as the Vice Dean of the School of Telecommunications Engineering, Xidian University. He has authored over 50 journal papers and 20 conference papers. His research interests include wideband wireless communications, signal processing for communications, and spatial communications networks.

Cheng-Xiang Wang (S'01–M'05–SM'08–F'17) received the B.Sc. and M.Eng. degrees in communication and information systems from Shandong University, China, in 1997 and 2000, respectively, and the Ph.D. degree in wireless communications from Aalborg University, Denmark, in 2004.

He was a Research Fellow with the University of Agder, Grimstad, Norway, from 2001 to 2005, a Visiting Researcher with Siemens AG Mobile Phones, Munich, Germany, in 2004, and a Research Assistant with the Hamburg University of Technology, Hamburg, Germany, from 2000 to 2001. He has been with Heriot-Watt University, Edinburgh, U.K., since 2005, where he was promoted to Professor in 2011. He has authored one book, one book chapter, and over 300 papers in refereed journals and conference proceedings. His current research interests include wireless channel modeling and (B)5G wireless communication networks, including green communications, cognitive radio networks, high mobility communication networks, massive MIMO, millimeter wave communications, and visible light communications.

Dr. Wang is a fellow of the IET and HEA, and a member of the EPSRC Peer-Review College. He received nine best paper awards from the IEEE Globecom 2010, the IEEE ICCT 2011, the ITST 2012, the IEEE VTC 2013, the IWCMC 2015, the IWCMC 2016, the IEEE/CIC ICCC 2016, and the WPMC 2016. He served or is serving as a TPC member, the TPC chair, and the general chair of over 80 international conferences. He was the Lead Guest Editor of the IEEE JOURNAL ON SELECTED AREAS IN COMMUNICATIONS Special Issue on Vehicular Communications and Networks. He served or is currently serving as an editor for nine international journals, including the IEEE TRANSACTIONS ON VEHICULAR TECHNOLOGY since 2011, the IEEE TRANSACTIONS ON COMMUNICATIONS since 2015, and the IEEE TRANSACTIONS ON WIRELESS COMMUNICATIONS from 2007 to 2009. He is also a Guest Editor of the IEEE JOURNAL ON SELECTED AREAS IN COMMUNICATIONS Special Issue on Spectrum and Energy Efficient Design of Wireless Communication Networks, and the IEEE TRANSACTIONS ON BIG DATA Special Issue on Wireless Big Data.

Rui Zhang received the B.S. and M.S. degrees in telecommunications engineering from Xidian University, Xi'an, China, in 2012 and 2015, respectively. He is currently pursuing the Ph.D. degree in communication and information system with Xidian University. He was a visiting Ph.D. student under the supervision of Professor C.-X. Wang with Heriot-Watt University, Edinburgh, U.K., from 2016 to 2017. His current research interests focus on device-to-device communications, vehicle-to-vehicle communications, radio resource allocation techniques, and energy efficient wireless networks.